

Recovering Robustness in Model-Free Reinforcement Learning

Harish K Venkataraman¹ and Peter J. Seiler²

Abstract—Reinforcement learning (RL) is used to directly design a control policy using data collected from the system. This paper considers the robustness of controllers trained via model-free RL. The discussion focuses on posing the (model-free) linear quadratic Gaussian (LQG) problem as a special instance of RL. A simple LQG example is used to demonstrate that RL with partial observations can lead to poor robustness margins. It is proposed to recover robustness by introducing random perturbations at the system input during the RL training. The perturbation magnitude can be used to trade off performance for increased robustness. Two simple examples are presented to demonstrate the proposed method for enhancing robustness during RL training.

I. INTRODUCTION

There has been rapid and impressive progress in machine learning in the past decade. One particular approach, reinforcement learning (RL) [21], [22], has close connections to optimal control techniques. RL is a model-free approach to directly design the control policy using data collected from the system via simulation or experiments. There have been several successful applications of RL on a variety of systems including helicopters [14] and robotics [18], [20], [10], [11].

This paper uses the standard model-based linear quadratic Gaussian (LQG) problem to explore the robustness of model-free RL controllers. The LQG problem, reviewed in Section II-A, is formulated with linear state-space models and an expected quadratic cost [12], [23]. The optimal controller is an observer/state-feedback with gains computed from two Riccati equations. We refer to this as “model-based” because the optimal controller is constructed explicitly using the state matrices. RL, reviewed in Section II-B, is a closely related problem formulated with partially observable Markov decision processes (POMDPs) and expected cumulative rewards [21], [22]. We refer to this as “model-free” because typical solution methods directly search for the control policy using simulation or experimental data.¹

RL with POMDPs is sufficiently general to solve the LQG problem as a special case, as discussed in Section II-C. This connection is motivated by recent work [19] which considers the linear quadratic regulator (LQR) as a special instance of RL with MDPs. Section III builds on [19] by exploring the robustness properties of model-free RL with POMDPs. First,

¹The boundaries between “model-based” and “model-free” are not necessarily well-defined. For example, the state matrices used in the LQG problem are often constructed from data using system identification techniques. We still call the LQG solution “model-based” as the construction of the optimal controller directly uses these state matrices. The sample complexity of such an approach is a subject of current research [4]. Conversely, an RL policy trained with simulation data implies the existence of a model, i.e. the simulator itself. We still call this “model-free” as the RL controller is constructed from data without directly using the model information.

Section III-A reviews a well-known example by Doyle [5] in which the optimal LQG controller has poor robustness margins. This is in contrast to LQR state feedback controllers which have provably good margins [1]. Section III-B finds (nearly) optimal policies for Doyle’s example using a simple RL method: policy search using gradient ascent and random initialization. With sufficient data, this policy search converges to the optimal LQG controller. This illustrates that model-free RL with POMDPs, as a special case of LQG, can also lead to controllers with poor robustness margins.

Small robustness margins indicate that the feedback system may become unstable due to small changes in the plant gain or parasitic dynamics. This has practical implications for model-free RL with POMDPs. Small robustness margins imply that an RL controller trained via simulation might lead to an unstable feedback system when implemented on the real plant. Alternatively, consider the scenario where the RL controller is trained via experimental data on a real physical device. The RL controller might cause instability if the dynamics of the system vary slightly over time. Moreover, the same RL controller might cause instability if implemented on other identical plants due to manufacturing tolerances, e.g. RL trained on one robot but implemented for production on many of the same type of robot.

Several methods were proposed to recover robustness in LQG regulators including loop transfer recovery [8], [9] and robust H_2 [17]. These issues also motivated the development of alternative synthesis and analysis techniques including H_∞ optimal control [7], μ analysis [6], [15], and DK synthesis [16]. All these approaches to address robustness issues can be characterized as model-based.

A key contribution of this paper is a model-free method to enhance robustness of RL controllers. This approach, discussed in Section III-C, consists of introducing random perturbations at the system input during the RL training phase. The specified level of input perturbation provides a tuning knob to trade-off performance for robustness. It is shown that this modification to RL training improves the robustness margins on Doyle’s example (Section III-C) and a simplified model of a flexible body (Section IV).

II. OPTIMAL CONTROL FORMULATIONS AND SOLUTIONS

A. Linear Quadratic Gaussian (LQG) Control

This section briefly reviews the LQG control problem and its solution. Additional details on LQG and the more general H_2 optimal control problem can be found in many textbooks, e.g. Chapter 6 of [12] and Chapter 14 of [23].

Consider a linear time-invariant, discrete-time system:

$$\begin{aligned} x_{t+1} &= Ax_t + Bu_t + B_w w_t \\ y_t &= Cx_t + v_t \end{aligned} \quad (1)$$

where $x \in \mathbb{R}^{n_x}$ is the state, $u \in \mathbb{R}^{n_u}$ is the control input, and $y \in \mathbb{R}^{n_y}$ is the measurement. The process noise $w \in \mathbb{R}^{n_w}$ and sensor noise $v \in \mathbb{R}^{n_v}$ are assumed to be white, zero mean, and Gaussian with variances $W := E[w_t w_t^T]$ and $V := E[v_t v_t^T]$. The (infinite-horizon) LQG optimal control problem is formulated using a quadratic cost:

$$J_{LQG}(u) := \lim_{N \rightarrow \infty} \frac{1}{N} E \left[\sum_{t=0}^N x_t^T Q x_t + u_t^T R u_t \right] \quad (2)$$

$Q \succeq 0$ and $R \succ 0$ are matrices that define penalties on the state and control input. The control inputs u_t are restricted to depend on past measurements, i.e. $u_t(y_0, \dots, y_{t-1})$.² The infinite-horizon LQG problem is to select these control inputs to minimize the cost J_{LQG} .

The infinite-horizon LQG problem includes additional technical assumptions, e.g. stabilizability of A and B . These additional assumptions ensure that an optimal solution exists and is given by the following estimator and state-feedback:

$$\begin{aligned} \hat{x}_{t+1} &= A\hat{x}_t + Bu_t + L(y_t - C\hat{x}_t) \\ u_t &= -K\hat{x}_t \end{aligned} \quad (3)$$

The matrices K and L are the optimal linear quadratic regulator (LQR) and Kalman filter gains. To compute these gains, let $DARE(A, B, Q, R)$ denote the discrete-time Algebraic Riccati Equation involving the matrix $X = X^T$:

$$X = A^T X A - A^T X B (R + B^T X B)^{-1} B^T X A + Q \quad (4)$$

Let P_c and P_e denote the stabilizing solutions to $DARE(A, B, Q, R)$ and $DARE(A^T, C^T, B_w W B_w^T, V)$, respectively. The LQR and Kalman filter gains are:

$$K := (B^T P_c B + R)^{-1} B^T P_c A \quad (5)$$

$$L := A P_e C^T (C P_e C^T + V)^{-1} \quad (6)$$

The optimal controller in Equation 3 exhibits the well-known separation principle: it consists of the optimal state-feedback gain coupled with an optimal state estimate. This is a model-based solution, i.e. a model of the plant dynamics (as given by A, B, C , etc.) is used to compute the gains and construct the controller in Equation 3. This is in contrast to the standard approaches for reinforcement learning which are data-driven.

B. Reinforcement Learning (RL)

This section briefly reviews reinforcement learning (RL). Some notation is chosen to align more closely with the LQG problem discussed in the previous section. Additional details on RL can be found in [21] and [22].

²This form assumes a one time-step delay from measurements at time $t - 1$ to the use for control at time t . This “delayed” form for LQG accounts for any processing and sensing delays in the feedback path. An alternative formulation assumes that u_t depends on measurements up to time t , i.e. $u_t(y_0, \dots, y_t)$. This “current” form for LQG allows (immediate) direct feedthrough in the control. This paper uses the “delayed” form but similar results can be obtained for the “current” form.

RL is used to design policies (controllers) for an agent interacting with its environment (system/plant). Most RL problems are formulated with a Markov Decision Process (MDP) which obey the Markovian state assumption: the current state along with future actions completely determine the future states. It is further assumed that the state is available for the agent (full state feedback). It will be useful to instead consider models that include observations with uncertainty. These are known as Partially Observable Markov Decision Processes (POMDPs) and are defined by:

- A set of states S ,
- A set of actions A ,
- A state transition probability, \mathcal{T}
- A reward function, $r : S \times A \rightarrow \mathbb{R}$,
- A set of observations O , and
- An observation probability, \mathcal{O} .

A POMDP models the interaction of an agent with its environment accommodating both process and measurement uncertainty. The environment at time t is in a state $s_t \in S$. The agent takes an action $a_t \in A$ and, as a result, the environment transitions to a new state s_{t+1} with probability $\mathcal{T}(s_{t+1} | s_t, a_t)$. This also generates a reward $r(s_t, a_t)$. Moreover, the agent receives an observation $o_t \in O$ with probability $\mathcal{O}(o_t | s_t, a_t)$. The state transition and observation probabilities capture random variations due to environmental disturbances and measurement noise respectively. The objective in (finite-horizon) RL is to select the sequence of actions to maximize the following expected cumulative reward:

$$J_{RL}(a) := E \left[\sum_{t=0}^N r(s_t, a_t) \right] \quad (7)$$

For MDPs the agent is assumed to have access to the full state at each time, i.e. $o_t = s_t$. In this case, the actions can be computed by policies $\pi : S \rightarrow A$ that map the state s_t to an action $a_t = \pi(s_t)$. This represents a deterministic policy but stochastic stationary policies can also be used. Standard RL techniques compute the policy using (simulated or experimental) data. There are a number of methods to construct policies that maximize the cumulative reward including value iteration, policy iteration, policy search, etc. These approaches are model free, i.e. they require no explicit knowledge of the distribution \mathcal{T} .

In the more general POMDP formulation, the agent only has access to observations o_t . These observations provide information on the state and action (s_t, a_t) based on the probability \mathcal{O} . The action a_t at time t is restricted to depend on past observations and actions, i.e. $a_t(o_0, \dots, o_{t-1}, a_0, \dots, a_{t-1})$. Many solution methods exist for RL with POMDPs. In some cases, they require the construction of a belief state (or estimate of the hidden state) from the observations.

C. Solving LQG as a Special Case of RL

The summary of RL in the previous subsection focused on finite-state POMDPs with a finite-horizon cumulative reward. This formulation, with a few minor extensions, is sufficiently

general to solve the LQG problem as a special case. This reformulation is motivated by [19] which solves for an linear quadratic regulator (LQR) state feedback as a special case of RL with MDPs.

First, the LQG dynamics can be modeled as a POMDP with state, action (control input), and observation (measurement) at time t given by x_t , u_t , and y_t . This requires continuous sets for these quantities: $S := \mathbb{R}^{n_x}$, $A := \mathbb{R}^{n_u}$, and $O := \mathbb{R}^{n_y}$. Thus the transition and observation probabilities \mathcal{T} and \mathcal{O} are given as probability density functions. Specifically, the LQG plant update (Equation 1) implies that the transition to state x_{t+1} given (x_t, u_t) is modeled by a Gaussian distribution with mean $Ax_t + Bu_t$ and variance $B_wWB_w^T$. Thus $\mathcal{T} \sim \mathcal{N}(Ax_t + Bu_t, B_wWB_w^T)$ ³. Similarly, the LQG measurement y_t given (x_t, u_t) is modeled by $\mathcal{O} \sim \mathcal{N}(Cx_t, V)$. The per timestep RL reward corresponding to the LQG problem is:

$$r_{LQG}(x_t, u_t) := -(x_t^T Q x_t + u_t^T R u_t) \quad (8)$$

This is simply the negative of the per timestep LQG cost. Section II-B described RL with a finite horizon cumulative reward (Equation 7). A discount factor can be introduced to ensure that the cumulative reward remains bounded as $N \rightarrow \infty$. Alternatively, the cost can be normalized by $\frac{1}{N}$. Normalization is used here to align with the infinite-horizon LQG problem. LQG, recast in the RL framework, corresponds to maximizing the following average reward:

$$J_{LQG}(u) := \lim_{N \rightarrow \infty} \frac{1}{N} E \left[\sum_{t=0}^N r_{LQG}(x_t, u_t) \right] \quad (9)$$

Section II-A summarizes the typical model-based LQG solution. As noted above, this standard approach requires specific knowledge of the model dynamics (A, B, C , etc). This approach should be used if such model data is available since it provides the optimal controller from simple linear algebra calculations. Alternatively, the LQG problem can be formulated, as discussed here, as a special case of RL with POMDPs. This allows for existing RL techniques to be used to compute model-free solutions to the LQG problem.

III. ROBUSTNESS OF RL CONTROLLERS

A. LQG Robustness Issues: Doyle's Example

This section reviews a well-known example by Doyle [5] to illustrate the robustness issues that can arise with LQG control. Consider the discrete-time LQG problem formulated in Section II-A with the following plant, noise, and cost data:

$$A := \begin{bmatrix} 1.1052 & 0.1105 \\ 0 & 1.1052 \end{bmatrix}, B := \begin{bmatrix} 0.0053 \\ 0.1052 \end{bmatrix}, B_w := \begin{bmatrix} 0.1105 \\ 0.1052 \end{bmatrix} \\ C^T := \begin{bmatrix} 1 \\ 0 \end{bmatrix}, Q := 10^3 \begin{bmatrix} 1 & \\ & 1 \end{bmatrix}, R := 1, W := 10^3, V := 1$$

This corresponds to a discretization of the continuous-time plant dynamics given in [5] with zero-order hold and sample

³Here \mathcal{T} is the probability density of x_{t+1} given (x_t, u_t) . $\mathcal{T} \sim \mathcal{N}(m, \Sigma)$ denotes that \mathcal{T} is given by the probability density function for a normal distribution with mean m and variance Σ .

time $T_s = 0.1$ sec. The optimal controller is the estimator and state feedback in Equation 3 with the gains:

$$K^T = \begin{bmatrix} 9.5193 \\ 10.2579 \end{bmatrix} \text{ and } L = \begin{bmatrix} 1.1297 \\ 1.0012 \end{bmatrix} \quad (10)$$

This achieves the optimal cost $J_{LQG} = 1.373 \times 10^5$.

The feedback system of the plant and LQG controller has classical gain margins of [0.9802, 1.0007]. Thus very small changes in the plant gain will cause instability. The feedback system also has very small phase margins of ± 0.070 deg. Thus any parasitic (unmodeled) dynamics will also cause instability. Finally, the symmetric disk margin m_d [2], [3] is another useful robustness indicator⁴. The symmetric disk margin for this example is $m_d = 1.0007$. This is consistent with the poor classical gain and phase margins.

A key point of Doyle's example is that LQG regulators can have arbitrarily small margins. This is in contrast to LQR state feedback controllers which have provably good margins [1]. The plant in Doyle's example is unstable with both eigenvalues at $z = 1.1052$. However, poor robustness margins can arise even if the plant is stable and minimum phase, e.g. as in [13]. See Section 8.3 of [1] for additional details on loss of robustness with observers. Methods to recover robustness in LQG regulators include loop transfer recovery [8], [9] and robust H_2 [17]. Robustness issues also motivated the development of alternative synthesis and analysis techniques including H_∞ optimal control [7], μ analysis [6], [15], and DK synthesis [16]. All these approaches can be characterized as model-based.

B. Solving Doyle's Example with RL

This section reconsiders Doyle's example within the RL framework. The environment (system) is modeled by the POMDP corresponding to the discretized dynamics from Doyle's example. It is assumed that the environment model is not directly available and the policy (controller) is constructed using only input-output data. This corresponds to the situation where data is collected either from simulations or from experiments. The reward is defined as in Equation 8 with the matrices Q and R given in the previous section.

The optimal LQG controller (Equation 3) has an observer / state-feedback structure with explicit dependence on the model data. In the RL framework, the policy should be parameterized without specific dependence on the model. The policy for Doyle's example will be parameterized as a second-order, output feedback system in companion form:

$$z_{t+1} = A_K(\theta)z_t + B_K(\theta)y_t \\ u_t = C_K(\theta)z_t \quad (11)$$

where

$$A_K(\theta) := \begin{bmatrix} 0 & \theta_1 \\ 1 & \theta_2 \end{bmatrix}, B_K(\theta) := \begin{bmatrix} 1 \\ 0 \end{bmatrix}, C_K^T(\theta) := \begin{bmatrix} \theta_3 \\ \theta_4 \end{bmatrix} \quad (12)$$

⁴The margin $m_d > 1$ defines a disk in the complex plane with diameter on the real axis $[\frac{1}{m_d}, m_d]$. The feedback system is stable for all gain and phase variations within this disk.

Each vector $\theta \in \mathbb{R}^4$ corresponds to a specific policy denoted by $K(\theta)$. Note, for later comparison, that the optimal LQG controller can be written in this companion form (via a state transformation) as:

$$\theta_{LQG} := [-0.1095 \quad -0.0491 \quad -21.02 \quad 23.21]^T \quad (13)$$

Algorithm 1 provides a method to maximize the expected cumulative reward via gradient ascent with random initialization. Define the search hypercube $\mathcal{H} \subset \mathbb{R}^4$ by $\mathcal{H}(\underline{\theta}, \bar{\theta}) := \{\theta \in \mathbb{R}^4 : \theta_k \leq \bar{\theta}_k \leq \theta_k, k = 1, \dots, 4\}$. The algorithm randomly (uniformly) samples this hypercube for an initial vector of policy parameters, θ . A gradient step is taken to move to a new parameter vector with higher expected cumulative reward. For simplicity, the algorithm uses a fixed number of gradient steps N_{ga} . The parameter vector is allowed to exit the initial hypercube \mathcal{H} during the gradient ascent. This entire process is repeated for N_{ri} random initializations. The (sub-)optimal parameter vector θ_{opt} and largest reward J_{opt} are returned. As noted previously, there are many alternative algorithms for RL with POMDPs. Gradient ascent with random initialization is used here because the simple implementation allows to focus on the robustness issues.

Steps 9 and 6 in Algorithm 1 compute the the reward J_{RL} and its gradient ∇J_{RL} . A typical implementation would estimate these values with sample means obtained from many simulations of the closed-loop environment with the policy $K(\theta)$. These estimates converge to their true values as the number of simulations tends to infinity. This step was simplified in our implementation of Algorithm 1 to allow for efficient studies with a large number of initializations. Specifically, the true expected reward and gradient were exactly computed in Steps 9 and 6 from the solutions of related Lyapunov equations. Details are given in the appendix. This abstraction of a true RL implementation avoids the need for running many simulations for each sample θ .

Algorithm 1 Gradient Ascent with Random Initialization

- 1: **Given:** Hypercube $\mathcal{H}(\underline{\theta}, \bar{\theta})$, number of initializations N_{ri} , gradient steps N_{ga} , and gradient stepsize η .
 - 2: **Initialize:** $J_{opt} = -\infty$, $\theta_{opt} = 0$
 - 3: **for** $i = 1, \dots, N_{ri}$ **do**
 - 4: Sample $\theta \in \mathcal{H}$ from random uniform distribution
 - 5: **for** $j = 1, \dots, N_{ga}$ **do**
 - 6: Evaluate gradient $\nabla J_{RL}(\theta)$
 - 7: Update $\theta \leftarrow \theta + \eta \nabla J_{RL}(\theta)$
 - 8: **end for**
 - 9: Evaluate reward $J_{RL}(\theta)$ obtained by new $K(\theta)$
 - 10: **if** $J_{RL}(\theta) > J_{opt}$ **then**
 - 11: Set $J_{opt} := J_{RL}(\theta)$ and $\theta_{opt} := \theta$
 - 12: **end if**
 - 13: **end for**
 - 14: **Return** J_{opt} and θ_{opt}
-

Doyle’s example was solved using Algorithm 1 with the exact (Lyapunov-based) calculation for J_{RL} and ∇J_{RL} . The

implementation used $N_{ri} = 3 \times 10^4$ random initializations and $N_{ga} = 100$ gradient steps for each initialization. The following hypercube was used for sampling:

$$\underline{\theta} := \begin{bmatrix} -0.2 \\ -0.2 \\ -40 \\ 0 \end{bmatrix} \quad \text{and} \quad \bar{\theta} := \begin{bmatrix} 0 \\ 0 \\ 0 \\ 40 \end{bmatrix} \quad (14)$$

The best policy computed at the end of the search was:

$$\theta_{opt} := [-0.0346 \quad -0.0687 \quad -20.3441 \quad 22.83]^T \quad (15)$$

The reward achieved by this sub-optimal policy is $J_{opt} = -1.488 \times 10^5$. This is only 8.3% larger than the cost achieved by the optimal LQG controller (accounting for the sign change). The search dimension \mathbb{R}^4 is relatively small and hence this method finds a nearly optimal controller.

The feedback system of the plant and RL policy has classical gain, phase, and symmetric disk margins of $[0.9633, 1.0109]$, ± 0.331 degs, and $m_d = 1.009$. The model for the environment (plant) dynamics was used to compute these margins. However, it is possible to estimate robustness margins only from data. These small margins again indicate that the feedback system may become unstable due to small changes in the plant gain or parasitic dynamics. This has practical implications for model-free RL. Small robustness margins imply that an RL controller trained via simulation might lead to an unstable feedback system when implemented on the real plant. Alternatively, consider the scenario where the RL controller is trained via experimental data on a real system. The same RL controller might cause instability if the dynamics of the system vary slightly over time. Moreover, the same RL controller might cause instability if implemented for production on many devices of the same type (e.g. RL trained on one robot but implemented for production on many of the same type of robot). In summary, LQG is a special case of RL and hence it follows that RL with POMDPs can also have poor robustness margins.

C. Recovering Robustness in RL

As noted above, typical algorithms to improve robustness are model based. It would be useful to have an easily implementable, data-driven method to recover robustness. Two options for enhancing robustness are to: (i) alter the POMDP dynamics used in the training process or (ii) modify the reward function. This section focuses on the first option but concludes with a brief comment on the second option.

Consider the feedback interconnection shown in Figure 1. This diagram shows a system (environment) in feedback with a controller (policy). The system is assumed to be modeled by a POMDP with process noise w and sensor noise v (or more generally by the state transition \mathcal{T} and observation \mathcal{O} probabilities). The additional box Δ will be used to introduce perturbations to the dynamics (model uncertainty) during the training phase. Temporarily assume that $\Delta = 1$, i.e. no model uncertainty. A standard RL training approach would evaluate the expected reward for the policy over the random process and sensor noise. One might conjecture that

robustness would be enhanced by increasing the process noise w during the training phase. In fact, the robustness margins become smaller for Doyle’s example as the process noise variance $W \rightarrow \infty$. This counterintuitive result emphasizes the distinction between process noise (which enters externally to the feedback system) and model uncertainty (which appears internally in the feedback system).

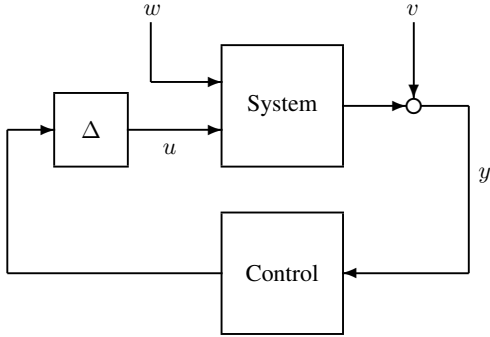


Fig. 1: RL Training With Input Perturbations

The proposed method to enhance robustness is to perform the training with random input perturbations. If the input is scalar then the perturbation in Figure 1 is set as $\Delta = 1 + \delta$ where δ is a uniform random variable in $[-b, b]$.⁵ The value $b > 0$ is selected to tune the amount of desired margin. The expected reward is computed over these input perturbations as well as the process and sensor noise. Thus the perturbations should be randomly sampled during each data collection. Such perturbations can be easily introduced during model-free RL training. They can be introduced when training either with simulations or with experimental devices. If the system has multiple inputs then a similar (independent) perturbation can be introduced into each input channel. The perturbation level b_i can be specified uniquely for channel i to obtain a desired robustness margin for that channel.

Gradient ascent was again applied to Doyle’s example with input perturbations at levels $b = 0$ (No perturbation), 0.1, 0.2, 0.3, 0.4. The algorithm parameters $(\mathcal{H}, N_{ri}, N_{ga}, \eta)$ were chosen the same as in the previous section. Figure 2 shows the disk margin versus the input perturbation percentage $(100 \times b)\%$. The algorithm was repeated 20 times for each input perturbation level. Each blue \times corresponds to one of these trials. The mean and \pm one standard deviation of these trial results are shown as cyan dashed lines. Finally, the disk margin for the optimal LQG controller $m_d = 1.0007$ is shown as the flat dashed red line. The disk margin increases with the input perturbation level b . Figure 3 shows the corresponding LQG costs (equal to the negative of the expected reward) versus the perturbation percent. This figure also shows the results for each of the one twenty trials (blue \times), mean and \pm one standard deviation over all trials (dashed cyan), and optimal LQG cost (red dashed at $J = 1.373 \times 10^5$). The cost increases (decreasing reward) as the input perturbation increases. This shows the expected

⁵Another alternative is to set Δ as a uniform random variable in $[\frac{1}{m}, m]$ where $m > 1$. This would align with the disk margin definition.

robustness versus performance trade-off. The perturbation level b provides a “knob” to easily make this trade-off.

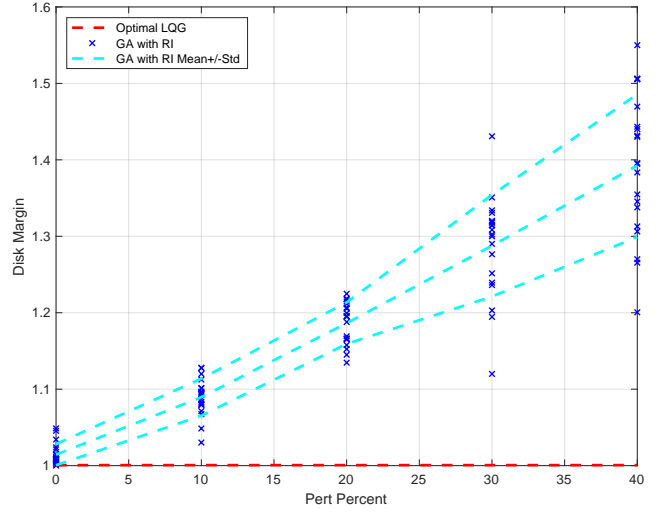


Fig. 2: Disk Margin vs Input Perturbation Percent ($100 \times b$)

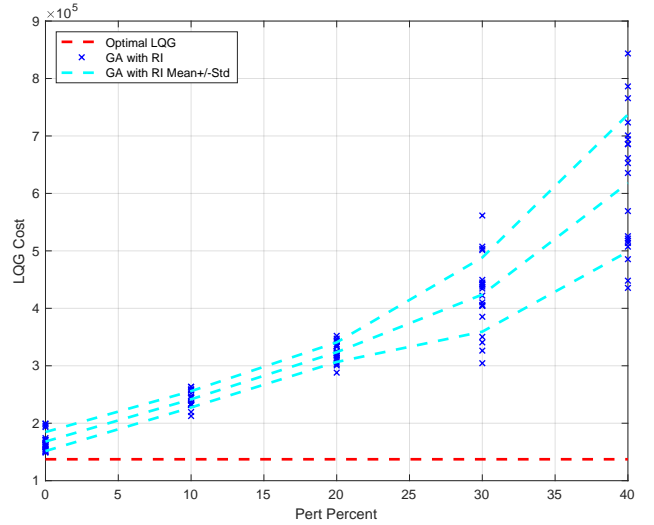


Fig. 3: LQG Cost vs Input Perturbation Percent ($100 \times b$)

To conclude this section, we briefly comment on the option to enhance robustness, in the RL framework, through proper modification of the reward function r . Consider the following per timestep reward for Doyle’s example:

$$r_{LQG}(x_t, u_t) := -(\sigma x_t^T \begin{bmatrix} 1 & 1 \\ 1 & 1 \end{bmatrix} x_t + u_t^T u_t) \quad (16)$$

If $\sigma = 1000$ then this corresponds to the reward used in the previous section to solve Doyle’s example in RL. This yielded small robustness margins. The margins become progressively smaller for $\sigma \rightarrow \infty$ as noted in [5]. Thus increasing the state penalty (or decreasing the control effort penalty) will further degrade robustness on this example. Conversely, robustness is enhanced on Doyle’s example by reducing the reward for good disturbance rejection. Trading

performance vs. robustness via properly modifying the reward function can be difficult or counter-intuitive in more complex problems. The input perturbation method described above provides a more direct means to improve robustness.

IV. EXAMPLE: SIMPLIFIED FLEXIBLE SYSTEM

This section considers a simplified flexible aircraft model drawn from [13], [1]. The model given in [1] is in continuous-time and represents a system with at low frequency rigid body mode at 1 rad/sec and a lightly damped flexible mode at 10rad/sec. The model also includes a coloring filter on the process noise with a bandwidth at 1 rad/sec. This idealized model can represent any system with a dominant low frequency rigid motion and high frequency flexible mode, e.g. a robotic system.

The continuous-time model was discretized with a zero-order hold and sample time $T_s = 0.09\text{sec}$. The corresponding plant, noise, and cost data for a discrete-time LQG problem (as formulated in Section II-A) is given by:

$$A := \begin{bmatrix} 0.9139 & 0 & 0 & 0.0823 \\ 0 & 0.6238 & 0.0776 & 0 \\ 0 & -7.7632 & 0.6083 & 0 \\ 0 & 0 & 0 & 0.9139 \end{bmatrix}$$

$$B := \begin{bmatrix} 0.0861 \\ 0.3762 \\ 7.7632 \\ 0 \end{bmatrix}, B_w := \begin{bmatrix} 0.0017 \\ 0 \\ 0 \\ 0.0387 \end{bmatrix}, C^T := \begin{bmatrix} 1 \\ 10 \\ 0 \\ 1 \end{bmatrix}$$

$$Q := \begin{bmatrix} 4 & 0 & 0 & 0 \\ 0 & 0 & 0 & 0 \\ 0 & 0 & 0 & 0 \\ 0 & 0 & 0 & 0 \end{bmatrix}, R := 1, W := 1, V := 0.01$$

The optimal LQG controller is the estimator and state feedback in Equation 3 with the following gains:

$$K = [1.1154 \quad 0 \quad 0 \quad 0.3976]$$

$$L^T = [0.0673 \quad 0 \quad 0 \quad 0.2496]$$

The optimal cost achieved by this LQG controller is $J_{LQG} = 0.0072$ and the disk gain margin is $m_d = 1.0091$. This small margin again indicates the poor robustness of the optimal (model-based) LQG controller for this system.

Standard RL can be used to construct controllers for this example as discussed in Section II-C. The policy is parameterized as a third-order system (as in Eq. 11) with state matrices in controllable canonical form:

$$A_K(\theta) := \begin{bmatrix} 0 & 1 & 0 \\ 0 & 0 & 1 \\ \theta_1 & \theta_2 & \theta_3 \end{bmatrix}, B_K(\theta) := \begin{bmatrix} 0 \\ 0 \\ 1 \end{bmatrix}, C_K^T(\theta) := \begin{bmatrix} \theta_4 \\ \theta_5 \\ \theta_6 \end{bmatrix}$$

Each vector $\theta \in \mathbb{R}^6$ corresponds to a specific policy denoted by $K(\theta)$. The gradient ascent in Algorithm 1 is applied with $N_{ri} = 10^4$ random initializations and $N_{ga} = 10^3$ gradient steps. The search hypercube $\mathcal{H}(\underline{\theta}, \bar{\theta})$ is defined by:

$$\underline{\theta} := [0 \quad -2 \quad 0 \quad -0.1 \quad 0 \quad -0.3]^T,$$

$$\bar{\theta} := [1 \quad 0 \quad 2 \quad 0 \quad 0.3 \quad 0]^T$$

These bounds were chosen with some trial and error. Most controllers in this search space are stable and minimum phase. In practice, some a priori knowledge would be required to obtain reasonable bounds on the search space.

Algorithm 1 was repeated for 25 trials with no input perturbations. The optimal controller found on these trials achieved a cost between 0.0075 and 0.0085. Thus the RL implementation converges to nearly optimal controllers. Small disk margins were obtained for these RL controllers with values ranging from 1.0131 to 1.31. Note that the optimal LQG controller is fourth-order and is not contained within the third-order parametrization used for RL. These results demonstrate that robustness issues in RL can still arise even with parameterizations that do not include the optimal LQG controller. This further motivates the need to recover robustness in the RL training.

The input perturbation method (Section III-C) was applied to this example with perturbation levels $b = 0$ (No perturbation), 0.1, 0.2, 0.3, 0.4. Figures 4 and 5 show the disk margins and LQG cost (= -reward) for this example. The input perturbation method was applied with the same N_{ri} , N_{ga} and hypercube $\mathcal{H}(\underline{\theta}, \bar{\theta})$ specified above. These figure shows the results for each of the twenty five trials (blue x), mean and \pm one standard deviation over all trials (dashed cyan), and for the optimal LQG controller (flat red dashed). Figure 4 shows the improvement in the disk margin robustness with increasing input perturbation level. Conversely, Figure 5 shows the degradation in performance with increasing input perturbation level. This again demonstrates that the perturbation level b can be used to trade off robustness and performance during the RL training.

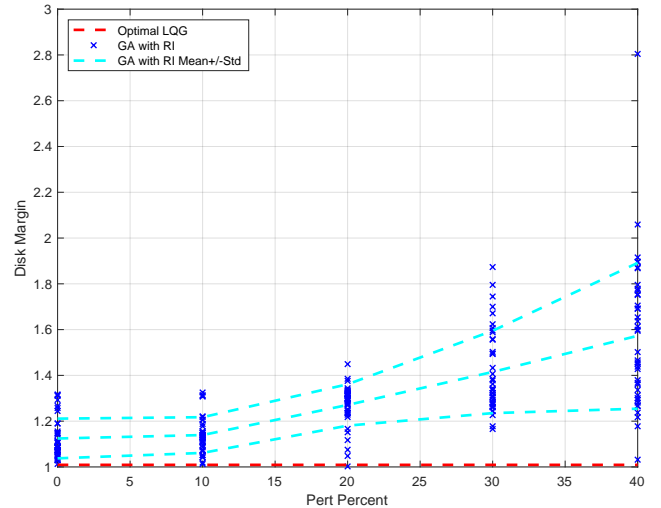


Fig. 4: Disk Margin vs Input Perturbation Percent ($100 \times b$)

V. CONCLUSION

Reinforcement learning (RL) with POMDPs is sufficiently general to solve the standard LQG problem. Thus LQG can be used to explore the robustness of RL controllers. A simple example by Doyle was used to demonstrate that

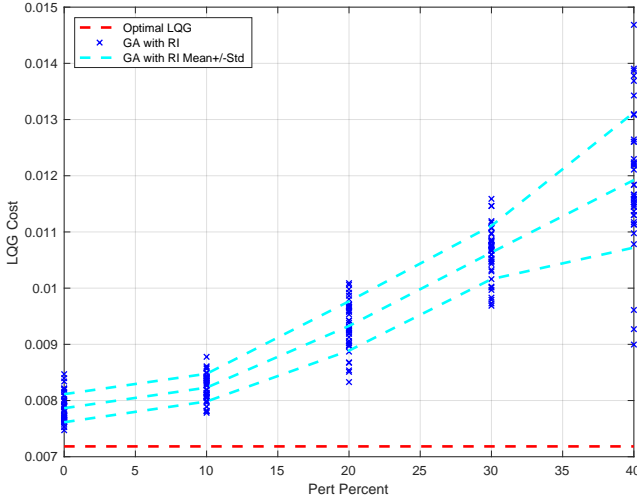


Fig. 5: LQG Cost vs Input Perturbation Percent ($100 \times b$)

RL with partial observations can lead to poor robustness margins. It is proposed to recover robustness by introducing random perturbations at the system input during the RL training. Two simple examples were used to demonstrate the effectiveness of this technique to trade off performance for robustness. Future work will explore the theoretical basis for the numerical results observed in this paper.

REFERENCES

- [1] B.D.O. Anderson and J. B. Moore. *Optimal Control: Linear Quadratic Methods*. Dover, 2007.
- [2] D. Bates and I. Postlethwaite. *Robust multivariable control of aerospace systems*. Delft University Press, 2002.
- [3] J. D. Blight, R. L. Dailey, and D. Gangsaas. Practical control law design for aircraft using multivariable techniques. *International Journal of Control*, 59(1):93–137, 1994.
- [4] S. Dean, H. Mania, N. Matni, B. Recht, and S. Tu. On the sample complexity of the linear quadratic regulator. *arXiv*, 2017.
- [5] J. Doyle. Guaranteed margins for lqg regulators, in *IEEE Transactions on Automatic Control*, 23(4):756–757, 1978.
- [6] J. Doyle. Analysis of feedback system with structured uncertainties. *IEE Proceedings D - Control Theory and Applications*, pages 242–250, 1982.
- [7] J.C. Doyle, K. Glover, P.P. Khargonekar, and B.A. Francis. State-space solutions to standard H_2 and H_∞ control problems. *IEEE Trans. on Aut. Control*, 34(8):831–847, 1989.
- [8] J.C. Doyle and G. Stein. Robustness with observers. *IEEE Trans. on Aut. Control*, 24(4):607–611, 1979.
- [9] J.C. Doyle and G. Stein. Multivariable feedback design: Concepts for a classical/modern synthesis. *IEEE Trans. on Aut. Control*, 26(1):4–16, 1981.
- [10] A. Gudimella, R. Story, M. Shaker, R. Kong, M. Brown, V. Shnayder, and M. Campos. Deep reinforcement learning for dexterous manipulation with concept networks. *arXiv*, 2017.
- [11] D. Kalashnikov, A. Irpan, P. Pastor, J. Ibarz, A. Herzog, E. Jang, D. Quillen, E. Holly, M. Kalakrishnan, V. Vanhoucke, and S. Levine. QT-Opt: Scalable deep reinforcement learning for vision-based robotic manipulation. *arXiv*, 2018.
- [12] H. Kwakernaak and R. Sivan. *Linear Optimal Control Systems*. Wiley, 1972.
- [13] J.B. Moore, D. Gangsaas, and J.D. Blight. Performance and robustness trades in lqg regulator design. In *IEEE Conference on Decision and Control*, pages 1191–1200, 1981.
- [14] A.Y. Ng, H. J. Kim, M. I. Jordan, and S. Sastry. Autonomous helicopter flight via reinforcement learning. In *Advances in Neural Information Processing Systems 16*, pages 799–806, 2004.

- [15] A. Packard and J. Doyle. The complex structured singular value. *Automatica*, 29(1):71–109, 1993.
- [16] A. Packard, J. Doyle, and G. Balas. Linear, multivariable robust control with a μ perspective. *Transactions of the ASME*, 115:426–438, 1993.
- [17] F. Paganini. Robust H_2 performance: Guaranteeing margins for lqg regulators. Technical Report CIT-CDS 95-031, CDS at California Institute of Technology, 1995.
- [18] J. Peters and S. Schaal. Policy gradient methods for robotics. In *IEEE/RSJ International Conference on Intelligent Robots and Systems*, pages 2219 – 2225, 2006.
- [19] B. Recht. A tour of reinforcement learning: The view from continuous control. *arXiv*, 2018.
- [20] F. Stulp, J. Buchli, E. Theodorou, and S. Schaal. Reinforcement learning of full-body humanoid motor skills. In *IEEE-RAS International Conference on Humanoid Robots*, pages 405 – 410, 2010.
- [21] R.S. Sutton and A.G. Barto. *Reinforcement Learning: An Introduction*. Bradford, 1998.
- [22] C. Szepesvari. *Algorithms for Reinforcement Learning*. Morgan and Claypool, 2010.
- [23] K. Zhou, J.C. Doyle, and K. Glover. *Robust and Optimal Control*. Pearson, 1995.

APPENDIX

Consider the following discrete-time system:

$$\bar{x}_{t+1} = \bar{A}\bar{x}_t + \bar{w}_t \quad (17)$$

where \bar{w}_t is white, zero mean, and Gaussian with variance $\bar{W} := E[\bar{w}_t\bar{w}_t^T]$. Assume \bar{A} is a Schur matrix, i.e. all eigenvalues have magnitude < 1 . There exists a unique solution $X \succeq 0$ to the discrete-time Lyapunov equation:

$$\bar{A}^T X \bar{A} - X + \bar{W} = 0 \quad (18)$$

The following steady-state relation holds for any matrix M :

$$\lim_{N \rightarrow \infty} \frac{1}{N} E \left[\sum_{t=0}^N \bar{x}_t^T M \bar{x}_t \right] = \text{trace}(MX) \quad (19)$$

The dynamics of the plant (environment) and controller (policy) can be combined to model the closed-loop system as in Equation 17. Moreover, the RL cumulative reward can be expressed as in Equation 19 for an appropriately chosen M . Thus this result can be used to exactly compute the closed-loop reward from the solution of the Lyapunov equation.

The gradient of the expected cumulative reward function can be obtained by evaluating the gradient of Equation 19. An application of the chain rule yields:

$$\nabla J_{RL}(\theta) = \text{trace}(\nabla M(\theta) \cdot X(\theta) + M(\theta) \cdot \nabla X(\theta)) \quad (20)$$

Assume that both $\nabla M(\theta)$ and $\nabla \bar{A}(\theta)$ can be computed. Then only $\nabla X(\theta)$ is needed in order to compute $\nabla J_{RL}(\theta)$. This is obtained by solving the following Lyapunov equation for ∇X (dropping the notational dependence on θ):

$$\bar{A}^T (\nabla X) \bar{A} - \nabla X + (\nabla \bar{A})^T X \bar{A} + \bar{A}^T X (\nabla \bar{A}) = 0 \quad (21)$$